Research Square

Preprints are preliminary reports that have not undergone peer review.
They should not be considered conclusive, used to inform clinical practice,
or referenced by the media as validated information.

Integrated Computer-Aided Drug Design Reveals Potential Hepatoprotective Phytoconstituents from Achyranthes aspera and Durantaerecta Dual Targeting Molecular Pathways Associated with Paracetamol-Induced Hepatotoxicity

Shreya Gupta
Mahatma Jyotiba Phule Rohilkhand University Bareilly
Pawan Kumar Gupta
Mahatma Jyotiba Phule Rohilkhand University Bareilly
Nandani Sharma
Mahatma Jyotiba Phule Rohilkhand University Bareilly
Kamini .
Mahatma Jyotiba Phule Rohilkhand University Bareilly
Yogesh Kumar
Mahatma Jyotiba Phule Rohilkhand University Bareilly
Shashi Bhooshan Tiwari
s.tiwari@mjpru.ac.in

Mahatma Jyotiba Phule Rohilkhand University Bareilly

Research Article

Keywords: In silico drug design, Hepatoprotective, Phytoconstituents, Achyranthes aspera, Durantaerecta

Posted Date: November 27th, 2026

DOI: https://doi.org/10.21203/rs.3.rs-11247015/v1

License: This work is licensed under a Creative Commons Attribution 4.0 International License.
Read Full License

Additional Declarations: No competing interests reported.

Research Paper

Integrated Computer-Aided Drug Design Reveals Potential Hepatoprotective Phytoconstituents from *Achyranthes aspera* and *Durantaerecta* Dual Targeting Molecular Pathways Associated with Paracetamol-Induced Hepatotoxicity

Shreya Gupta[1], Pawan Kumar Gupta[1], Nandani Sharma[1], Kamini[1], Yogesh Kumar[1], Shashi Bhooshan Tiwari[1*]

[1]Department of Pharmacy Mahatma Jyotiba Phule Rohilkhand University Bareilly, Uttar Pradesh India 243006

***Corresponding Author:**
Prof. Shashi Bhooshan Tiwari
Department of Pharmacy, MJP Rohilkhand University, Bareilly, Uttar Pradesh, India 243006
Contact no. 9451325149
Email: s.tiwari@mjpru.ac.in

Graphical Abstract:

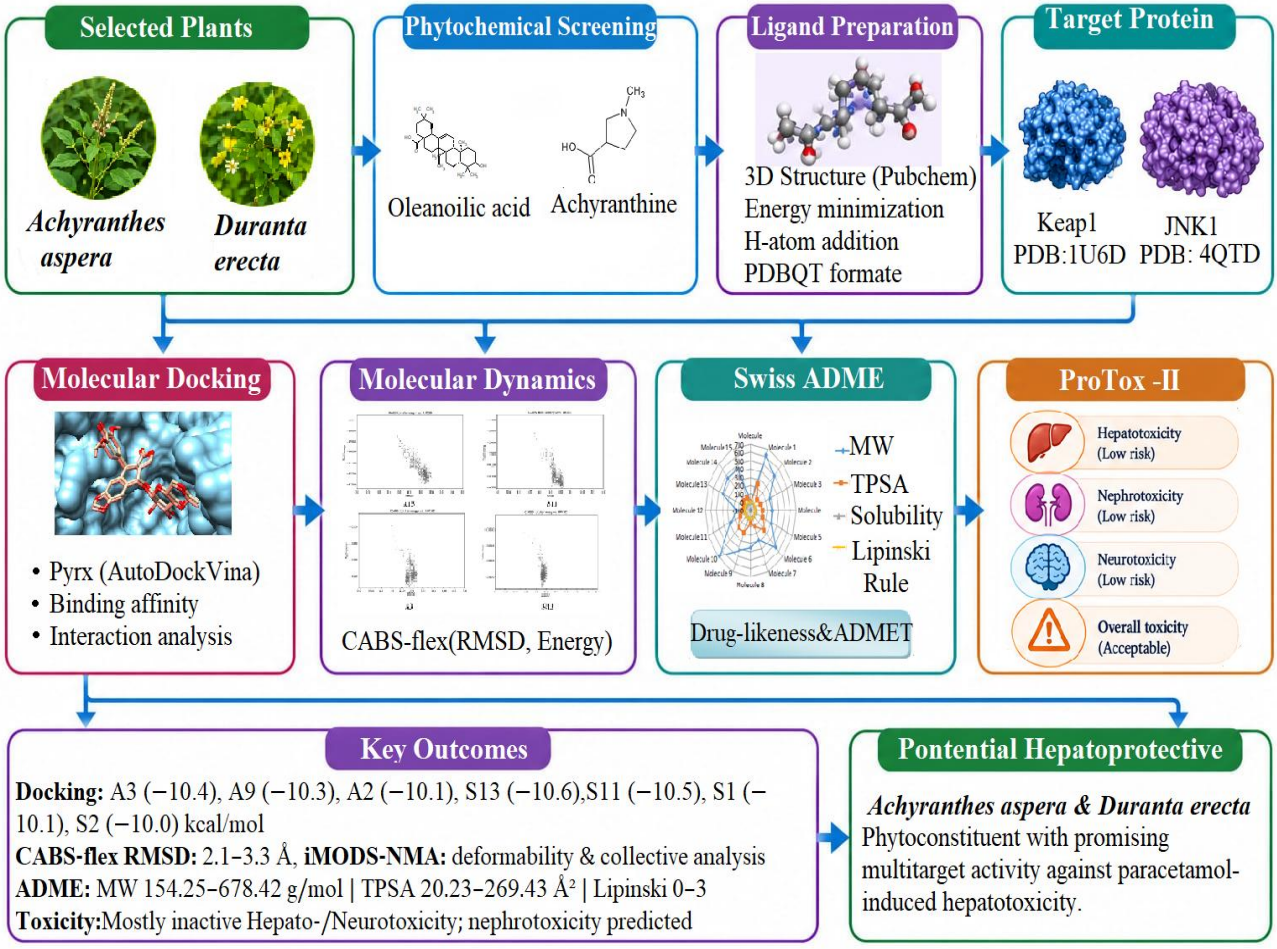

Abstract:

Paracetamol-induced hepatotoxicity is a major cause of drug-induced liver injury and involves oxidative stress, inflammatory signaling, mitochondrial dysfunction, and apoptosis. Medicinal plants provide diverse phytoconstituents with potential multitarget pharmacological activity; however, their molecular interactions with proteins associated with hepatotoxicity remain insufficiently characterized. The present study employed an integrated computer-aided drug design approach to investigate potential hepatoprotective phytoconstituents from *Achyranthes aspera* and *Durantaerecta*. Selected phytoconstituents were evaluated against Kelch-like ECH-associated protein 1 (Keap1; PDB ID: 1U6D) and c-Jun N-terminal kinase 1 (JNK1/MAPK8; PDB ID: 4QTD) using molecular docking, followed by interaction analysis. The predicted docking affinities ranged from −8.7 to −10.6 kcal/mol, while the reference compounds showed affinities ranging from −9.7 to −10.7 kcal/mol. Among the investigated compounds, A3, A9, A2, and S13 exhibited favorable interactions with 1U6D, whereas S11, S1, and S2 demonstrated favorable binding with 4QTD through hydrogen bonding and other non-covalent interactions. CABS-flex analysis showed clustered conformational distributions for the selected complexes, while iMODS-based normal mode analysis provided complementary information on deformability, collective motions, covariance, and elastic-network characteristics. SwissADME analysis revealed molecular weights of 154.25–678.42 g/mol, TPSA values of 20.23–269.43 Å², and 0–3 Lipinski rule violations. ProTox-II prediction indicated predominantly inactive hepatotoxicity and neurotoxicity profiles, although nephrotoxicity was predicted for several compounds. Overall, the integrated computational findings identify selected phytoconstituents from *A. aspera* and *D. erecta* as promising candidates for further hepatoprotective investigation. Experimental validation is warranted to confirm their pharmacological activity, mechanism of action, and safety.

Key words: *In silico drug design***,** Hepatoprotective, Phytoconstituents, *Achyranthes aspera, Durantaerecta*

1. Background:

The liver is the biggest internal organ and is the key metabolic centre of the body, which performs a variety of physiological functions significant for maintaining homeostasis in the organism. The liver is involved in the regulation of carbohydrate, lipid, and protein metabolism, synthesis of the plasma proteins and factors for blood coagulation, in the storage of gases, vitamins, and minerals, and in the biotransformation and detoxification of both endogenous metabolites and xenobiotics. Due to its anatomical features and constant interaction with food, environmental and pharmaceutical agents the liver is prone to the action of toxic agents. Damage of hepatocytes due to the impact of medicines, alcoholic drinks, infective agents, metabolic disorders and environmental toxins poses a large health problem globally and makes a substantial contribution to high morbidity, mortality, and healthcare costs. Even though modern medicine has made some progress, the opportunities to prevent and treat liver diseases are still limited [1-6].

DILI is known as one of the most common causes of acute liver failure across the globe, and because of that many therapeutic drugs have been pulled off from the market and different clinical stages. Among different tested drugs which are responsible for liver toxicity, it can be seen that paracetamol is one of the most commonly used drugs causing acute liver injury. Although paracetamol is considered a safe medication, its overdose may lead to severe centrilobular liver necrosis and its swift development into acute liver failure. Moreover, paracetamol-induced liver toxicity is also considered the best model for testing different mechanisms of liver damage and clinical evaluation of new hepatoprotective drugs [7-9].

The cause behind the liver toxicity caused by paracetamol is that the body uses biochemical and molecular processes that are complex. In healthy conditions, around 90% of paracetamol taken undergoes different processes including glucuronidation or sulphation - a process that produces harmless compounds that get removed through urine. Some amount of this compound is metabolised by cytochrome enzymes (CYP2E1, CYP1A2, and CYP3A4) and turned into a very reactive intermediate called NAPQI. With the right therapeutic use of paracetamol, NAPQI is detoxified through a reaction with glutathione. However, too much intake of paracetamol means that GSH is not produced and too much NAPQI is produced in the body that results in liver damage[10,11]**.**

Oxidative stress constitutes a central mechanism underlying paracetamol-induced liver injury. Excessive generation of reactive oxygen species (ROS) overwhelms endogenous antioxidant defence systems, including superoxide dismutase (SOD), catalase (CAT), glutathione peroxidase (GPx), and glutathione reductase. Increased oxidative stress promotes mitochondrial dysfunction, DNA damage, protein oxidation, membrane lipid peroxidation, and activation of stress-responsive signalling pathways. These molecular events subsequently stimulate inflammatory cascades through activation of transcription factors such as nuclear factor-kappa B (NF-κB), resulting in increased production of pro-inflammatory cytokines including tumour necrosis factor-alpha (TNF-α), interleukin-1β (IL-1β), and interleukin-6 (IL-6). Persistent inflammation further amplifies hepatocellular injury and contributes to progressive liver dysfunction [12,13].

Apoptosis is also involved in hepatotoxicity caused by paracetamol. The activation of JNK pathway along with the event of mitochondrial permeability transition, cytochrome c release

and activation of caspases promote the occurrence of programmed cell death. At the same time, the disruption of Nrf2 antioxidant pathway reduces cell resistance towards oxidative injury. The Keap1-Nrf2 signaling pathway has thus become one of the important targets in the prevention of liver damage linked to oxidative stress. The inhibition of CYP2E1 and suppression of certain inflammatory factors (NF-κB and TNF-α) should also be considered as efficient ways of preventing hepatotoxicity caused by drugs [14-16].

At the moment, the only antidote approved by the medical community to treat paracetamol poisoning is N-acetylcysteine (NAC). However, NAC is very successful when the drug is administered soon after overdose ingestion, and its effectiveness is severely reduced as the time of administration delays. There are negative effects like nausea, vomiting, hypersensitivity, and anaphylactoid reactions of NAC usage, resulting in the search for new hepatoprotective substances, which can show better efficacy and safety. It has been the reason for the rise in the interest of the scientific world in the medicinal plants that have gained their popularity for a long time, as many plants contain lots of active ingredients that show antioxidant, anti-inflammatory, anti-apoptotic, and cytoprotective activity[17,18].
Historically, therapeutic use of medicinal plants has provided humans with treatment for several diseases. Nearly 80% of the world's population still turns to herbal remedies in their quest for treatment, specifically in underdeveloped and developing countries. The biological activity of plant-derived secondary metabolites includes flavonoids, phenolic acids, alkaloids, terpenoids, saponins, glycosides, tannins, and steroids, which are able to target various molecular targets at the same time. Phytochemicals are superior in comparison with many synthetic drugs, which usually act on one particular target, and can thus be used to treat cumbersome issues such as liver injury.

Achyranthesaspera L. (Family: Amaranthaceae), commonly known as prickly chaff flower, is a medicinal herb widely distributed throughout tropical and subtropical regions. The plant occupies an important place in traditional Ayurvedic, Siddha, and folk medicine systems, where it has been used for centuries to manage inflammation, fever, wounds, diabetes, asthma, renal disorders, and hepatic ailments. Phytochemical investigations have identified numerous bioactive constituents including oleanolic acid, ursolic acid, ecdysterone, β-sitosterol, quercetin, kaempferol, rutin, saponins, alkaloids, flavonoids, and phenolic compounds. Experimental studies have demonstrated that extracts of *A. aspera* possess antioxidant, anti-inflammatory, antimicrobial, immunomodulatory, nephroprotective, antidiabetic, and hepatoprotective activities. The hepatoprotective effects are primarily attributed to its ability to scavenge reactive oxygen species, restore endogenous antioxidant enzymes, inhibit lipid peroxidation, and modulate inflammatory signalling pathways [19,20].

Durantaerecta L. (Family: Verbenaceae), commonly referred to as golden dewdrop or pigeon berry, is another medicinal plant extensively employed in traditional medicine. Different parts of the plant have been reported to exhibit antimicrobial, antioxidant, antiviral, anti-inflammatory, analgesic, antidiabetic, anticancer, and hepatoprotective properties. Phytochemical analyses have revealed the presence of flavonoids, phenylethanoid glycosides such as acteoside and verbascoside, chlorogenic acid, caffeic acid, luteolin, apigenin, quercetin, iridoids, and triterpenoids. These phytoconstituents possess potent free radical scavenging and anti-inflammatory activities and have demonstrated protective effects against oxidative tissue

damage in various experimental models. Their ability to regulate inflammatory mediators and enhance antioxidant defence mechanisms suggests significant therapeutic potential in preventing paracetamol-induced hepatic injury [21-23].

Over the last few years, significant advancements in computational biology and computer-aided drug design have revolutionized drug discovery by allowing drug developers to identify and optimize potential drug candidates quickly. In silico approaches such as molecular docking, molecular dynamics simulation, pharmacokinetic prediction, toxicity assessment, and network pharmacology help predict molecular interactions of bioactive compounds with targeted disease-related proteins before laboratory testing. These methods lead to a drastic reduction in the periods, costs, and resources required by classic drug development as well as an increase in the chances of finding promising lead compounds. Among various computational techniques, molecular docking has become one of the most widely employed methods for predicting ligand–protein interactions. Docking algorithms estimate the preferred binding orientation of phytochemicals within the active site of target proteins and calculate binding affinities that reflect the stability of protein–ligand complexes. Analysis of hydrogen bonding, hydrophobic interactions, π–π stacking, electrostatic interactions, and amino acid residues involved in binding provides valuable insights into potential mechanisms of action. In hepatoprotective drug discovery, molecular docking can identify phytoconstituents capable of modulating proteins implicated in oxidative stress, inflammation, apoptosis, and xenobiotic metabolism, including CYP2E1, Keap1, and JNK [24-26].

In addition to molecular docking, computational evaluation of drug-likeness and pharmacokinetic properties has become indispensable during lead optimisation. Lipinski's Rule of Five, Veber's criteria, SwissADME, pkCSM, and ADMETlab platforms provide valuable information regarding oral bioavailability, gastrointestinal absorption, blood–brain barrier permeability, cytochrome P450 interactions, toxicity profiles, and predicted biological activities. These in silico tools facilitate the prioritisation of phytochemicals with favourable pharmacological characteristics before undertaking expensive in vitro and in vivo investigations. Despite numerous reports describing the hepatoprotective activities of *Achyranthesaspera* and *Durantaerecta* individually, comparative computational investigations evaluating their phytoconstituents against multiple molecular targets involved in paracetamol-induced liver injury remain limited. Furthermore, there is insufficient integration of phytochemical screening, molecular docking, drug-likeness evaluation, ADMET prediction, and mechanistic target analysis to identify the most promising bioactive molecules responsible for their hepatoprotective effects. Addressing these gaps could accelerate the discovery of novel plant-derived lead compounds for the prevention and treatment of drug-induced liver injury [27-29].

Therefore, the present study is designed to investigate the hepatoprotective potential of phytoconstituents from *Achyranthesaspera* and *Durantaerecta* using an integrated in silico drug design approach. By employing molecular docking against key proteins implicated in paracetamol-induced hepatotoxicity, together with drug-likeness assessment and ADMET prediction, the study aims to identify bioactive compounds with favourable binding characteristics and pharmacokinetic profiles. The findings are expected to provide mechanistic insights into the molecular basis of the hepatoprotective activity of these medicinal plants and

establish a scientific foundation for future *in vitro, in vivo*, and clinical investigations directed towards the development of safe and effective plant-derived hepatoprotective therapeutics.

2. Research Gap

Even though there has been substantial conventional use and increasing experimental evidences supporting the hepatoprotective effects of Achyranthes aspera and Durantaerecta, there are still significant gaps in knowledge when it comes to understanding their pharmacological mechanisms. The majority of the available literature has focused on the phytochemical compounds and the in vitro and in vivo assessment using the experimentally induced liver injury models, such as paracetamol-induced liver damage. Though positive results have been obtained with respect to the development of biochemical parameters, enzymes activity, and liver histopathology without detailed information on active phytochemicals involved in the hepatoprotective effects exploration.

From an *in silico* drug design perspective, there is a notable scarcity of comprehensive computational studies investigating the phytoconstituents of *Achyranthesaspera* and *Durantaerecta* against proteins implicated in paracetamol-induced hepatotoxicity. Existing computational investigations are generally restricted to isolated compounds or single protein targets and rarely employ an integrated computer-aided drug design (CADD) workflow. Consequently, the molecular basis of ligand–target recognition, binding affinity, interaction stability, and target selectivity of these phytochemicals remains inadequately characterized [30,31].

Another important gap is the limited evaluation of multiple therapeutic targets involved in the pathogenesis of paracetamol-induced liver injury. Hepatotoxicity is a multifactorial process involving oxidative stress, inflammatory signalling, mitochondrial dysfunction, apoptosis, and xenobiotic metabolism. However, previous computational studies have seldom explored the multitarget potential of phytochemicals against key proteins such as cytochrome P450 2E1 (CYP2E1), Kelch-like ECH-associated protein 1 (Keap1), c-Jun N-terminal kinase (JNK). Since phytochemicals often exert therapeutic effects through simultaneous modulation of multiple signalling pathways, identification of multitarget lead compounds remains an important unmet research need.

Furthermore, although molecular docking has become an indispensable tool in natural product-based drug discovery, many published studies do not extend beyond docking score analysis. Advanced computational techniques such as molecular dynamics (MD) simulation, binding free-energy estimation (MM/PBSA or MM/GBSA), and dynamic stability analysis are infrequently incorporated. As a result, the long-term stability of protein–ligand complexes and the reliability of predicted binding interactions remain insufficiently validated.

A further limitation of the available literature is the inadequate assessment of pharmacokinetic and toxicity characteristics during early-stage lead identification. Drug-likeness evaluation based on Lipinski's Rule of Five, Veber's criteria, bioavailability prediction, and comprehensive ADMET (Absorption, Distribution, Metabolism, Excretion, and Toxicity) profiling are often omitted. Consequently, phytoconstituents exhibiting favourable binding affinity may possess poor oral bioavailability, undesirable metabolic characteristics, or potential toxicity, limiting their translational potential as drug candidates [32].

One more significant gap is related to the comparative study of medicinal plants. Even though Achyranthesaspera and Durantaerecta are acknowledged to possess hepatoprotective plant compounds, there are still no direct comparative computational studies regarding their bioactive ingredients based on the same molecular targets and standardized docking techniques.

In addition, the recent developments in the field of artificial intelligence, drug discovery, network pharmacology, and systems pharmacology demonstrated the need of conducting an analysis of complex interactions of phytochemical compounds with their targets. However, despite this wide range of opportunities in modern computing techniques, the investigation of the characteristics of Achyranthesaspera and Durantaerecta has not been performed yet.

As a result, there is an evident need for an all-inclusive in silico drug designing process that assimilates phytochemical screening, molecular docking, interaction analysis, drug-likeness analysis, ADMET prediction, biological activity prediction, and where applicable molecular dynamics simulation. This integrated computational approach will allow the identification of important hepatoprotective lead compounds from Achyranthesaspera and Durantaerecta, offer some mechanistic understanding with regards to the interaction of these compounds with proteins responsible for paracetamol-induced toxicity in the liver, and lay a solid scientific background for further in vitro, in vivo and clinical studies. By filling in these gaps, we will be able to help with sustainable development of novel hepatoprotective agents from plants with the use of modern information technologies in drug designing [33,34].

3. Materials and Methods

3.1 Study Design

The present study employed an integrated computer-aided drug design (CADD) approach to evaluate the hepatoprotective potential of phytoconstituents isolated from *Achyranthesaspera* and *Durantaerecta* against proteins implicated in paracetamol-induced hepatotoxicity. The computational workflow consisted of phytochemical selection, ligand preparation, target protein retrieval and preparation, molecular docking, molecular interaction analysis, drug-likeness evaluation, pharmacokinetic and toxicity prediction (ADMET), biological activity prediction, and molecular dynamics simulation of the most promising protein–ligand complexes [35,36].

3.2 Selection of Phytoconstituents

Major Phytochemicals reported from *Achyranthesaspera* and *Durantaerecta* were identified through a comprehensive review of peer-reviewed literature and phytochemical databases. The compounds selected for computational analysis included flavonoids, triterpenoids, phenolic acids, iridoids, sterols, and phenylethanoid glycosides based on their reported antioxidant, anti-inflammatory, and hepatoprotective properties, as shown in table 1.

Table 1: Representative Phytoconstituents analysed in the study

S. No.	Name	Structure

Achyranthesaspera		
1.	**Oleanoilic acid (A1)**	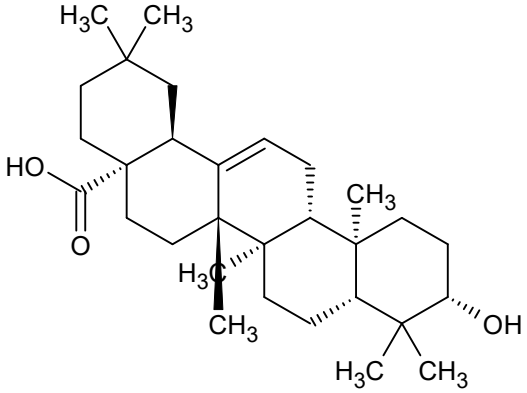
2.	**Ursolic acid (A2)**	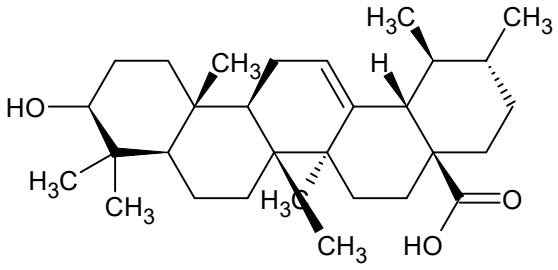
3.	**Beta-Ecdysterone (A3)**	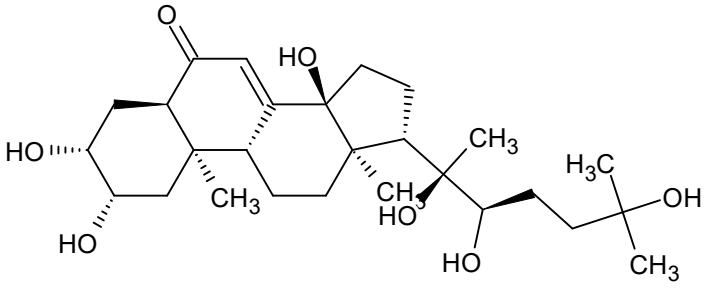
4.	**Achyranthine (A4)**	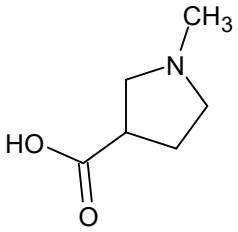

5.	**Beta-Sitosterol (A5)**	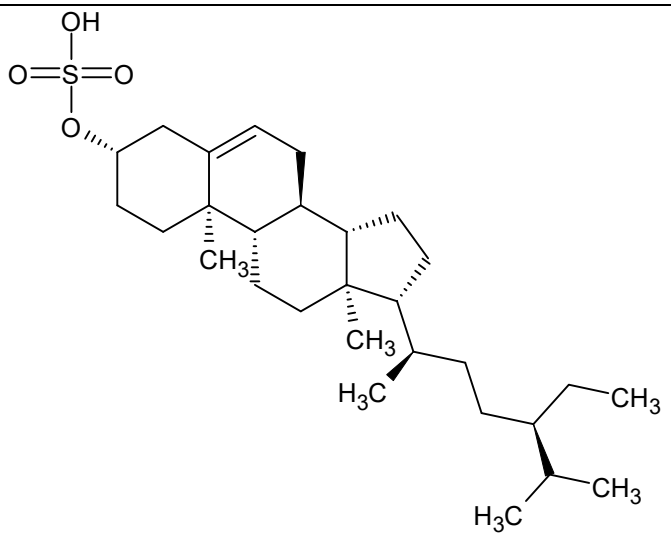
6.	**Rutin (A6)**	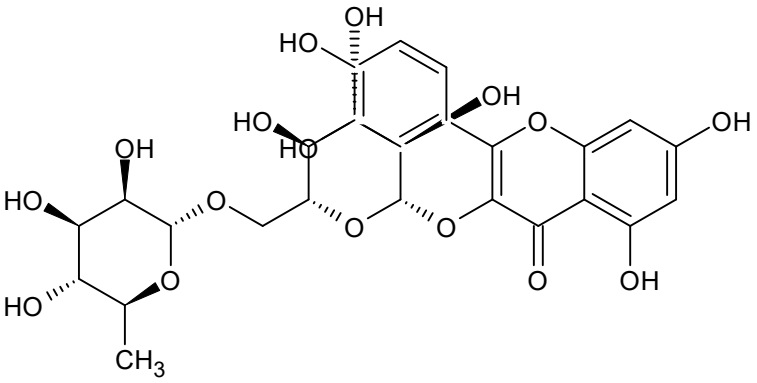
7.	**Genestein (A7)**	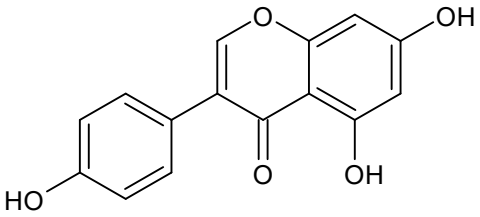
8.	**Taxifolin (A8)**	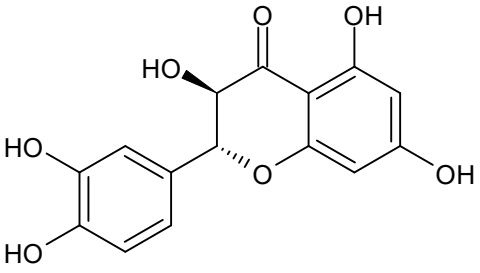

9.	**Kaempferol (A9)**	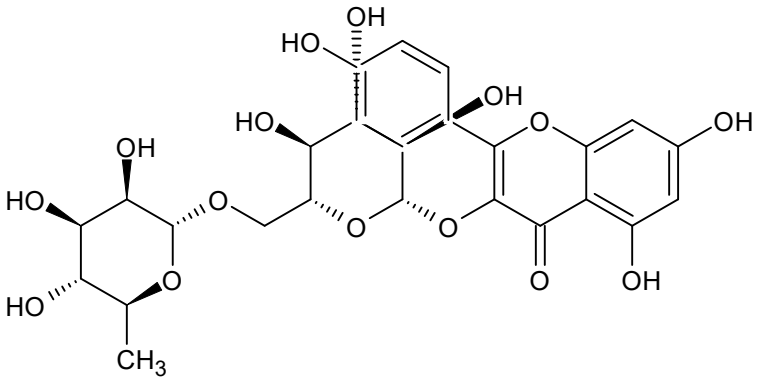
10.	**Nerol (A10)**	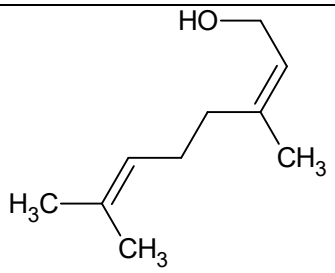
11.	**Gallic Acid (A11)**	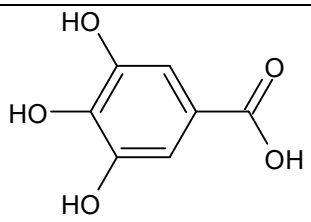
12.	**Vanillic acid (A12)**	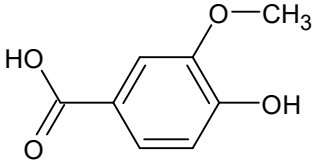
13.	**Chrysin (A13)**	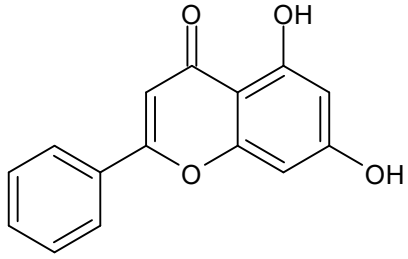
14.	**Ferulic Acid (A14)**	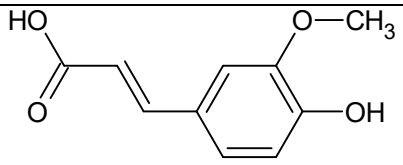

15.	**Quercetin (A15)**	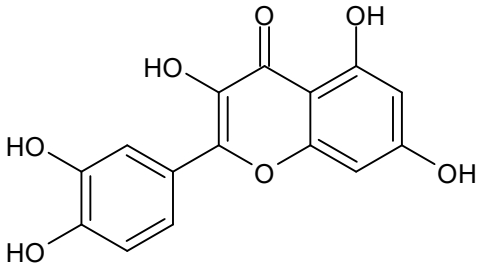
Durantaerecta		
1.	**Acetoside (S1)**	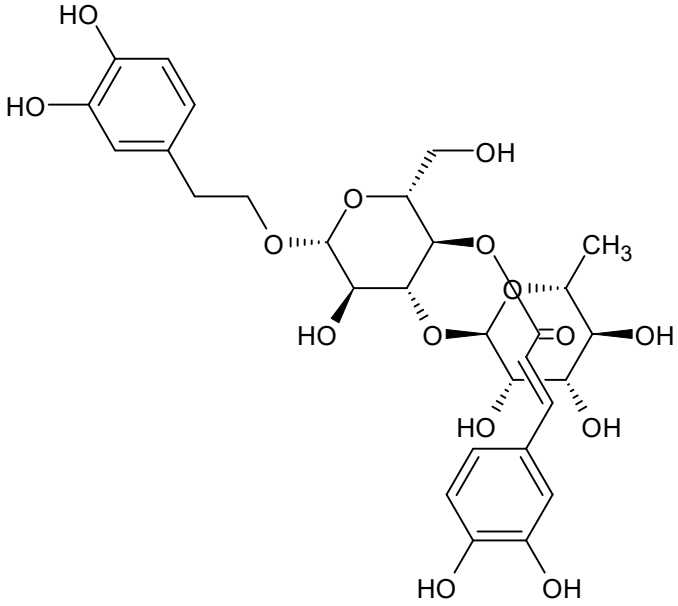
2.	**Beta-Sitosterol (S2)**	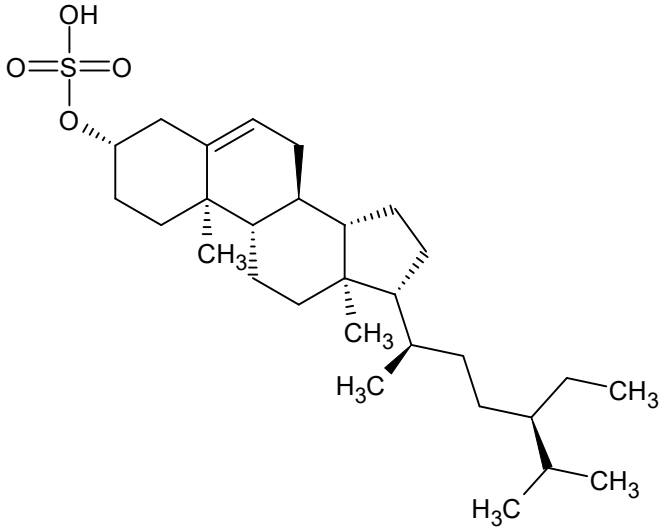
3.	**Apegenin (S3)**	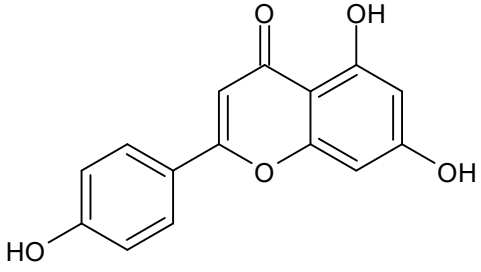

4.	**Luteolin (S4)**	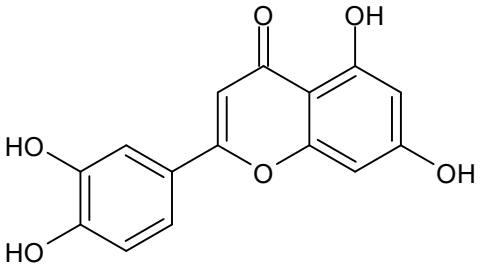
5.	**Quercetin (S5)**	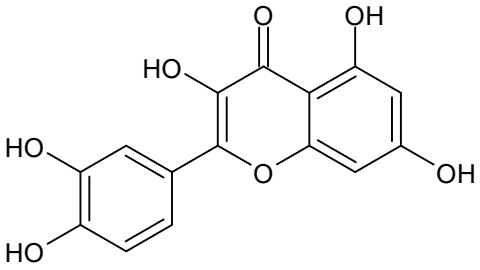
6.	**Chloregenic acid (S6)**	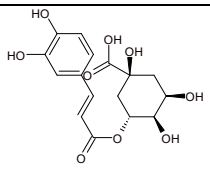
7.	**Caffeic Acid (S7)**	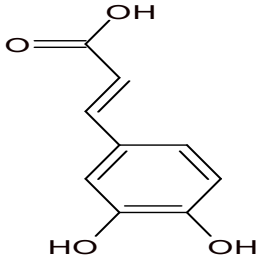
8.	**Scutellarein (S8)**	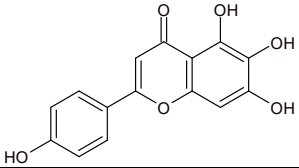
9.	**Phenyl ethanoic acid (S9)**	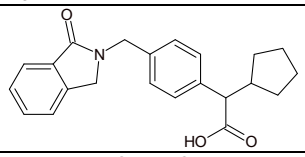
10.	**Lamiide (S10)**	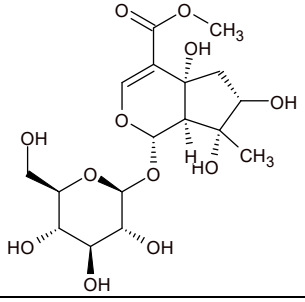

11.	**Durantoside (S11)**	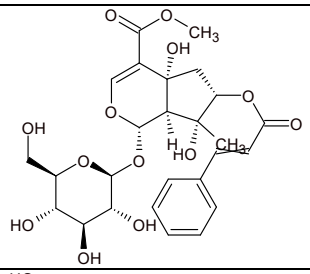
12.	**Naringenin (S12)**	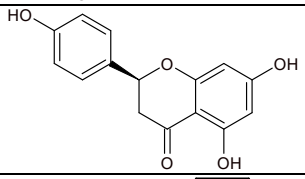
13.	**Cinnamic acid (S13**	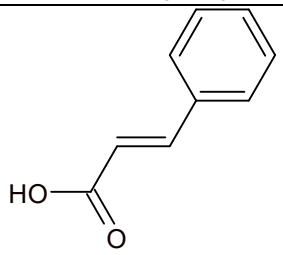
14.	**Alpha-Amyrin (S14)**	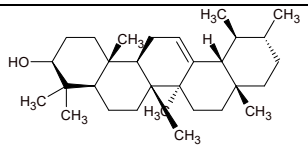
15.	**Oleanolic acid (S15)**	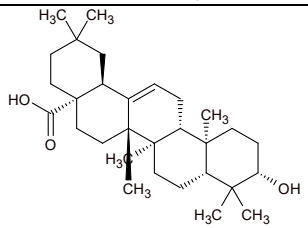

3.3 Ligand Preparation

The three-dimensional structures of all phytoconstituents were retrieved from the PubChem database in SDF format. The chemical structures were imported into Open Babel and converted into PDB format.Energy minimisation of each ligand was performed using the MMFF94 force field in Avogadro to obtain energetically favourable conformations. Hydrogen atoms were added, bond orders were corrected, and Gasteiger charges were assigned before molecular docking. The optimised ligands were finally saved in PDBQT format using AutoDock Tools.

3.4 Selection of Target Proteins

Proteins associated with the molecular pathogenesis of paracetamol-induced hepatotoxicity were selected based on published literature.



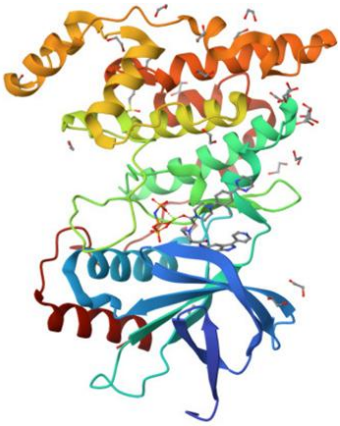

Keap1 Regulation of Nrf2 **JNK1(MAPK8)**

PDB ID: 1U6D **PDB ID: 4QTD**

Figure 1: Three-dimensional structures of the selected target proteins: (A) Keap1 involved in Nrf2 regulation (PDB ID: 1U6D) and (B) JNK1/MAPK8 (PDB ID: 4QTD).

3.5 Protein Preparation

Protein preparation was carried out using UCSF Chimera and AutoDock Tools.

The following pre-processing steps were performed:

- Removal of co-crystallised ligands
- Removal of water molecules
- Addition of polar hydrogen atoms
- Assignment of Kollman charges
- Correction of missing residues (where applicable)
- Energy optimisation of the protein structure

Prepared proteins were exported in PDBQT format for docking studies.

3.6 Active Site Identification

The active binding sites of each target protein were identified using the coordinates of co-crystallised ligands available in the Protein Data Bank. For proteins lacking native ligands, binding pockets were predicted using CASTp and validated through published literature.

Grid boxes covering the active-site residues were generated using AutoDock Tools.

3.7 Molecular Docking

Molecular docking studies were performed using **PyRx** integrated within the PyRx virtual screening platform.

Docking parameters included:

- Exhaustiveness: 8
- Number of binding modes: 10

- Energy range: 3 kcal/mol

Each ligand was docked independently against every target protein.

Binding affinity was expressed as binding free energy (kcal/mol). Lower (more negative) docking scores indicated stronger predicted binding affinity.

3.8 Molecular Interaction Analysis

The best docking poses were selected according to the lowest binding energy and visualised using BIOVIA Discovery Studio Visualizer.

Protein–ligand interactions analysed included:

- Hydrogen bonding
- Hydrophobic interactions
- van der Waals interactions
- π–π stacking
- π–alkyl interactions
- Electrostatic interactions
- Amino acid residues participating in ligand binding

Interaction maps were generated to identify key residues responsible for ligand stabilisation within the binding pocket.

3.9 Molecular Dynamics Simulation

Normal mode analysis (NMA) and coarse-grained flexibility analysis were performed to investigate the structural mobility, flexibility, and conformational dynamics of the selected InhA–ligand complexes using the iMODS server (https://imods.iqf.csic.es/) and CABS-flex 2.0 (https://biocomp.chem.uw.edu.pl/CABSflex2), respectively. Unlike conventional all-atom molecular dynamics (MD) simulations, these approaches employ coarse-grained and elastic-network-based models to characterize macromolecular motions while reducing computational requirements. iMODS performs normal mode analysis using internal coordinates, particularly torsional degrees of freedom, to characterize collective motions and conformational changes within macromolecular structures. In the iMODS framework, the protein structure is represented using an elastic network model in which interacting structural elements are connected through harmonic potentials. The resulting normal modes provide information regarding the intrinsic flexibility, collective motions, deformability, and energetic characteristics of the investigated protein–ligand complexes. The analysis provides parameters such as root-mean-square deviation (RMSD), residue mobility profiles, deformability, eigenvalues, covariance matrices, and deformation trajectories, which collectively facilitate the assessment of structural dynamics and flexibility. CABS-flex 2.0 was additionally employed to evaluate residue-level fluctuations and conformational flexibility of the selected complexes using a coarse-grained simulation approach. The predicted conformational ensembles and flexibility profiles obtained from CABS-flex were used to complement the iMODS analysis and provide further insights into the dynamic behaviour of the protein–ligand complexes

[37,38]. Collectively, iMODS-based normal mode analysis and CABS-flex simulations provided complementary information on protein flexibility, collective motions, and conformational stability, thereby supporting the structural interpretation of the molecular docking results.

3.10 ADMET Profiling

The absorption, distribution, metabolism and excretion (ADME) characteristics of the selected phytoconstituents were evaluated using their physicochemical and pharmacokinetic descriptors, including molecular weight (MW), hydrogen-bond acceptors (HBA), hydrogen-bond donors (HBD), molar refractivity (MR), topological polar surface area (TPSA), rotatable bonds, gastrointestinal (GI) absorption, bioavailability score, blood–brain barrier (BBB) permeability and Lipinski rule violations.

3.11 Data Analysis

A summary of docking scores, physicochemical features, ADMET parameters, PASS predictions, and molecular dynamics descriptors was provided. In terms of their overall computational performance, the phytochemicals were arranged in order of efficacy based on binding affinity, the interaction profile, pharmacokinetic properties, and predicted activity. Those compounds that demonstrated the most favourable performance were marked as potential leads for the future pursuit of experimental studies.

4. Result and discussion

4.1 Molecular docking

Molecular docking analysis was performed to evaluate the binding interaction of the selected compounds with the target proteins 1U6D and 4QTD. The docking scores of the investigated compounds ranged from −8.7 to −10.6 kcal/mol, while the reference standards showed binding affinities of −9.7 to −10.7 kcal/mol. Several compounds exhibited conventional hydrogen-bond interactions with residues located within the respective binding pockets, together with π-associated and alkyl interactions.

For PDB ID 1U6D, Compound A3 showed a binding affinity of −10.4 kcal/mol and formed conventional hydrogen bonds with Ile X:416, Val X:463, Val X:606, and Gly X:367. Compound A9 showed a binding affinity of −10.3 kcal/mol, with conventional hydrogen-bond interactions involving Val X:465, Val X:512, Val X:608, and Leu X:557, along with carbon-hydrogen-bond interactions with Gly X:367 and Gly X:419. Compound A2 exhibited a binding affinity of −10.1 kcal/moland showed multiple hydrogen-bond and π-alkyl interactions involving Val X:465, Gly X:367, Val X:606, Val X:463, Ile X:416, Gly X:364, Gly X:603, Ala X:366, Ala X:556, Arg X:415, and Val X:418. Compounds A15 and A1 showed binding affinities of −10.0 kcal/mol, whereas A6 exhibited −9.8 kcal/mol, (fig. 2)**.**

Among the compounds listed for the *Durantaerecta* series, S13 showed a binding affinity of −10.6 kcal/mol, with conventional hydrogen-bond interactions involving Thr X:560, Ile X:559, Val X:561, Val X:606, Val X:465, Val X:418, Ile X:416, Gly X:367,and Leu X:365. Compound S3 showed −9.5 kcal/mol with hydrogen-bond interactions involving Ile X:416, Val X:418, Val X:465, and Ala X:510. S5 exhibited −9.4 kcal/mol, while S4 showed −9.3 kcal/mol. S10 and S8 displayed binding affinities of −8.8 kcal/mol (Table 2)**.**

For PDB ID 4QTD, several compounds demonstrated interactions with residues such as Gln A:37, Lys A:55, Val A:40, Val A:158, Ile A:32, Ala A:53, Leu A:168, Asn A:156, Asp A:151, Arg A:69, and Glu A:73**.** Compound S11 showed a binding affinity of −10.5 kcal/mol and formed conventional hydrogen bonds with Gln A:37, Lys A:55, and Met A:111, together with π-associated interactions involving Val A:40, Val A:158, Ile A:32, Ala A:53, and Leu A:168. Compound S1 showed −10.1 kcal/mol, with hydrogen bonding involving Gln A:37 and Lys A:55and π-associated interactions with Val A:40, Val A:158, Ile A:32, Ala A:53, and Leu A:168**.** Compound S2 exhibited −10.0 kcal/mol and formed multiple conventional hydrogen bonds involving Asn A:156, Lys A:55, Arg A:69, Asp A:151, Gln A:37, and Glu A:73 (fig.3).

The reference compounds also showed appreciable binding affinities. Standard 1 exhibited docking scores of −9.7 kcal/mol with 1U6D and −10.7 kcal/mol with 4QTD, while Standard 2showed −10.0 kcal/mol with 1U6Dand −9.7 kcal/mol with 4QTD. These interactions included conventional hydrogen bonding as well as π-sigma, π-sulfur, π-alkyl, and additional non-covalent contacts.

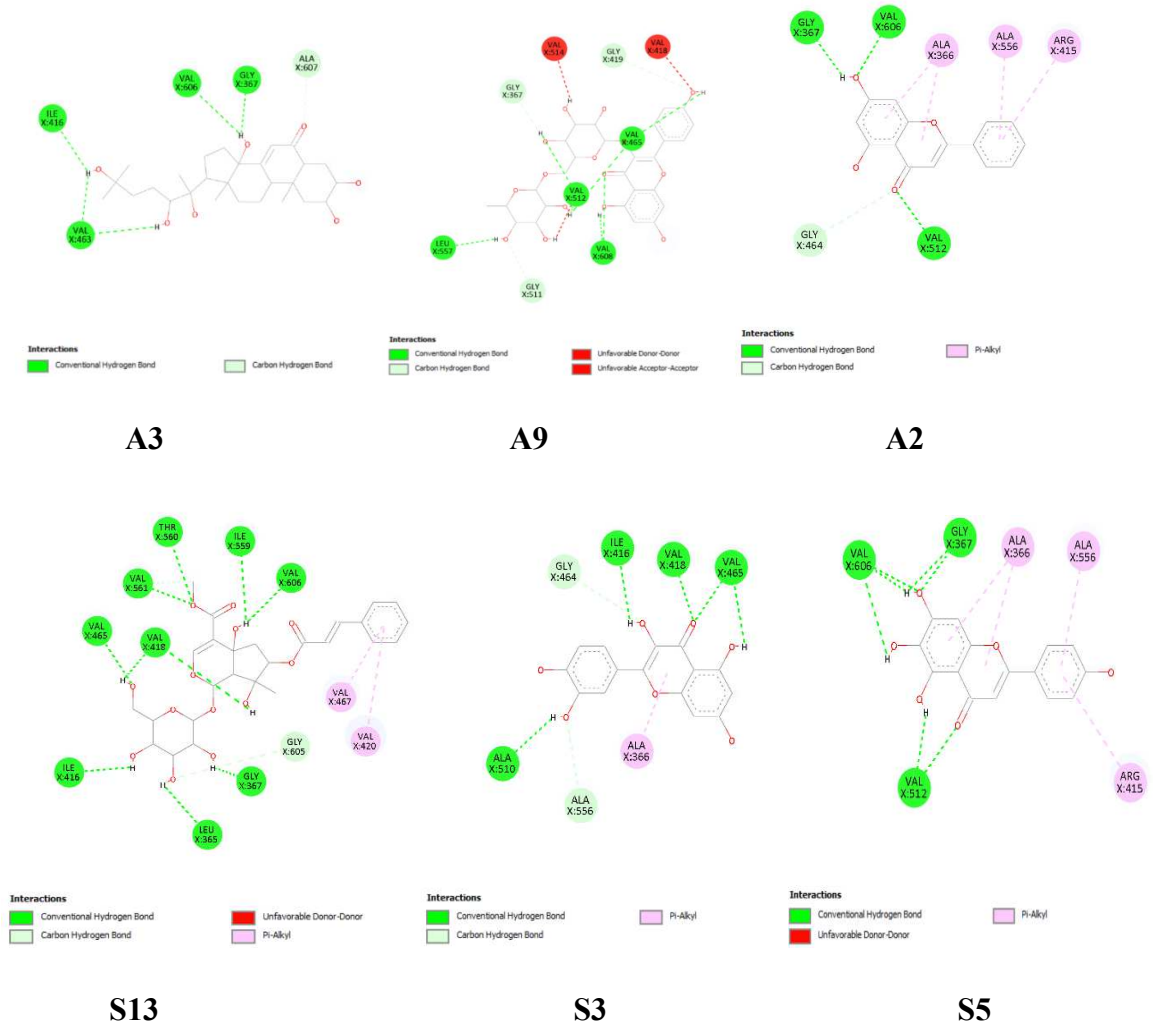

Figure 2: 2D chemical structures of selected *Achyranthes aspera* compounds (A3, A9, A2) and *Durantaerecta* compounds (S13, S3, and S5) showing favorable docking interactions with the target protein (PDB ID: 1U6D).

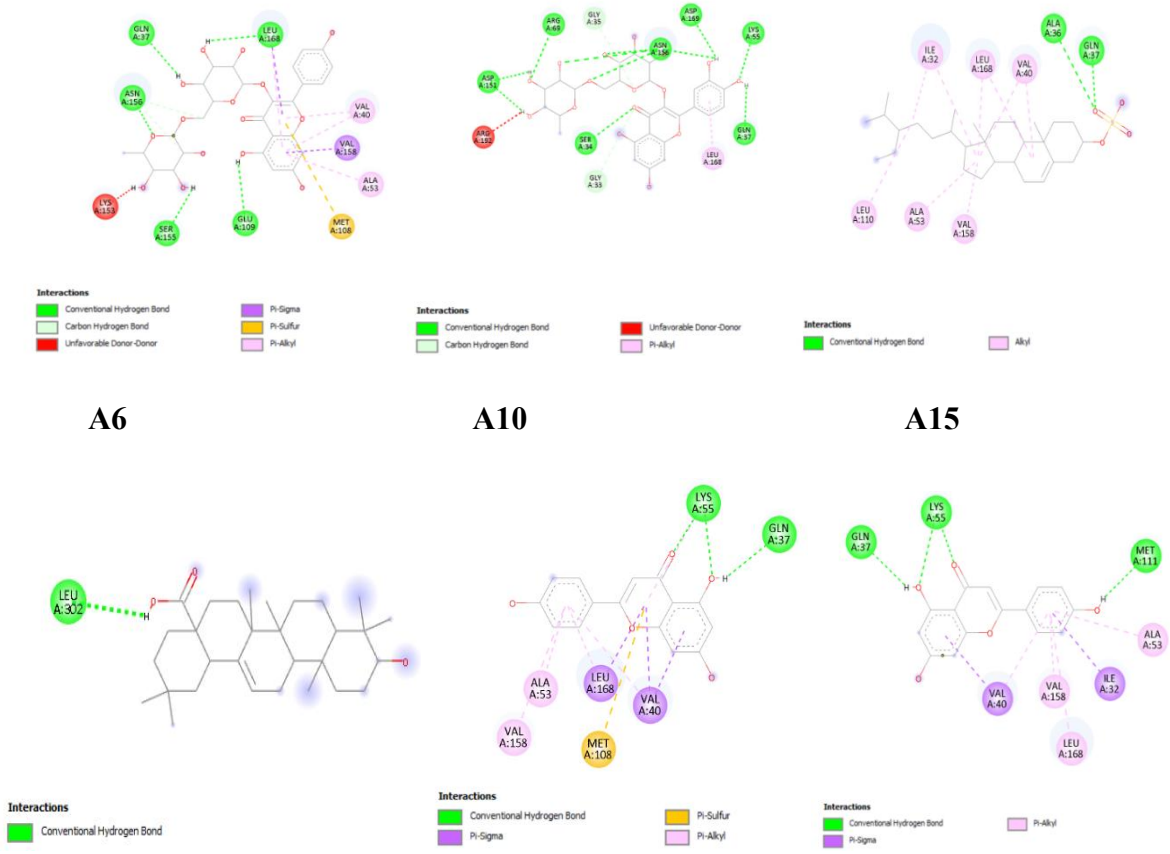

Figure 3: 2D chemical structures of selected *Durantaerecta* compounds (A15, A6, A10, S11, S1, and S3) showing favorable docking interactions with the target protein (PDB ID: 4QTD).

Table 2.Values represent predicted docking binding affinities (kcal/mol). H-bond, π-associated, π-alkyl, π-sigma, and π-sulfur interactions represent the major non-covalent interactions identified between the compounds and target proteins.

Compound	**Binding affinity (kcal/mol)**	**Key interactions with target protein**			
Achyranthesaspera					
PDB ID:1U6D			**PDB ID: 4QTD**		
Compound A3	**-10.4**	Conventional H-bond: Ile X:416, Val X:463, Val X:606, Gly X:367	**Compound A15**	**-10**	Conventional H-bond: Thr X:560, Ile X:559, Val X:561, Val X:606, Val X:465, Val X:418, Ile X:416, Gly X:367, Leu X:365

Compound A9	**-10.3**	Conventional H-bond: Val X:465, Val X:512, Val X:608, Leu X:557; Carbon H-bond: Gly X:367, Gly X:419; Unfavorable interactions: Val X:514 (Donor–Donor), Val X:418 (Acceptor–Acceptor)	**Compound A6**	**-9.8**	Conventional H-bond: Ile X:416, Val X:418, Val X:465, Ala X:510
Compound A2	**-10.1**	Conventional H-bond: Val X:465, Gly X:367, Val X:606; Carbon H-bond: Val X:463, Ile X:416, Gly X:364, Gly X:603, Ala X:366; π-Alkyl interactions: Ala X:556, Arg X:415, Val X:418	**Compound A10**	**-9.7**	Conventional H-bond: Val X:605, Gly X:367, Val X:512; π-associated interactions: Ala X:366, Ala X:556, Arg X:415.
Compound A1	**-10**	Conventional H-bond: Val X:467	**Compound A7**	**-9.3**	Conventional H-bond: Val X:465, Val X:512; unfavorable interaction: Val X:606; π-associated interactions: Arg X:415, Ala X:366, Ala X:556.
Compound A6	**-9.8**	Conventional H-bond: Ile X:559, Val X:465, Val X:418, Val X:365	**Compound A5**	**-8.7**	Conventional H-bond: Val X:606; unfavorable interaction: Ile X:559; π-associated interactions: Ala X:556, Gly X:464, Ala X:366, Cys X:513.
Durantaerecta					
Compound S13	**-10.6**	Conventional H-bond: Thr X:560, Ile X:559, Val X:561, Val X:606, Val X:465, Val X:418, Ile X:416, Gly X:367, Leu X:365.	**Compound S11**	**-10.5**	Conventional H-bond:Gln A:37, Lys A:55, Met A:111. **π-**associated interactions: Val A:40, Val A:158, Ile A:32, Ala A:53, Leu A:168.

Compound S3	**-9.5**	Conventional H-bond: Ile X:416, Val X:418, Val X:465, Ala X:510	**Compound S1**	**-10.1**	Conventional H-bond:Gln A:37, Lys A:55. π-associated interactions: Val A:40, Val A:158, Ile A:32, Ala A:53, Leu A:168.
Compound S5	**-9.4**	Conventional H-bond: Val X:605, Gly X:367, Val X:512; π-associated interactions involving Ala X:366, Ala X:556, Arg X:415	**Compound S2**	**-10**	Conventional H-bond:Asn A:156, Lys A:55, Arg A:69, Asp A:151, Gln A:37, Glu A:73. Unfavorable interaction:Arg A:192. Additional interactions:Leu A:168, Asp A:169.
Compound S4	**-9.3**	Conventional H-bond: Val X:465, Val X:512; unfavorable interaction involving Val X:606; additional π-associated interactions with Arg X:415, Ala X:366, Ala X:556	**Compound S9**	**-9.9**	π-Alkyl interactions: Ala A:53, Val A:158, Val A:40, Leu A:168, Ile A:32, Lys A:55.
Compound S10	**-8.8**	Conventional H-bond: Val X:606; unfavorable interaction with Ile X:559; additional π-associated interactions with Ala X:556, Gly X:464, Ala X:366, Cys X:513, Ala X:466	**Compound S8**	**-8.8**	Conventional H-bond:Leu A:62.
Standard 1	**-9.7**	Conventional H-bond: Val X:467, Val X:561, Gln X:563, Val X:561, Val X:465; additional interactions involving His X:516,	**Standard 1**	**-10.7**	π-Sigma interactions: Leu A:168, Val A:40, Ile A:32. π-Sulfur interaction: Met A:108. π-Alkyl interaction: Val A:158. Additional residues: Ala A:53, Gln A:117, Ala A:113.

		Gly X:564, Thr X:560			
Standard 2	**-10**	Conventional H-bond: Ile X:416, Val X:418, Val X:561, Thr X:557; additional interactions with Ala X:366, Val X:420, Val X:369, Gly X:558	**Standard 2**	**-9.7**	Conventional H-bond: Asn A:156, Asn A:111, Asp A:111. Carbon Hydrogen Bond: Ile A:32.

4.2 Molecular Dynamics Simulation

To further investigate the conformational stability and dynamic behavior of the selected ligand–protein complexes, CABS-flex 2.0 simulation and iMODS-based normal mode analysis (NMA) were performed for the selected complexes. The complexes A15 and S11 with PDB ID 4QTDandA3 and S13 with PDB ID 1U6D were subjected to comparative dynamic analysis.

The CABS total energy versus RMSD plots showed a distinct clustering of conformations for all the investigated complexes. For the 4QTD–A15 complex, the conformations were predominantly clustered at an RMSD of approximately 2.5–3.3 Å, with the major population concentrated around 3.0–3.3 Å and lower total-energy values approaching approximately −4200 to −4300. The 4QTD–S11 complex showed a similar clustering pattern, with most conformations distributed around 2.5–3.1 Å RMSD and predominantly lower total-energy values in the region of approximately −4200 to −4300. The formation of compact clusters at lower energy indicates the sampling of relatively stable conformational states during the simulation (fig.4,5).

For the 1U6D complexes**,** theA3–1U6D complex exhibited a major conformational cluster at approximately 2.3–2.9 Å RMSD, with total-energy values mainly distributed around −3400 to −3550**.** Similarly, the S13–1U6D complex showed a concentrated population of conformations around approximately 2.1–2.6 Å RMSD, with the predominant energy distribution occurring around −3450 to −3550. The relatively compact distribution of the sampled conformations suggests that the complexes maintained defined conformational states throughout the CABS-flex simulation.

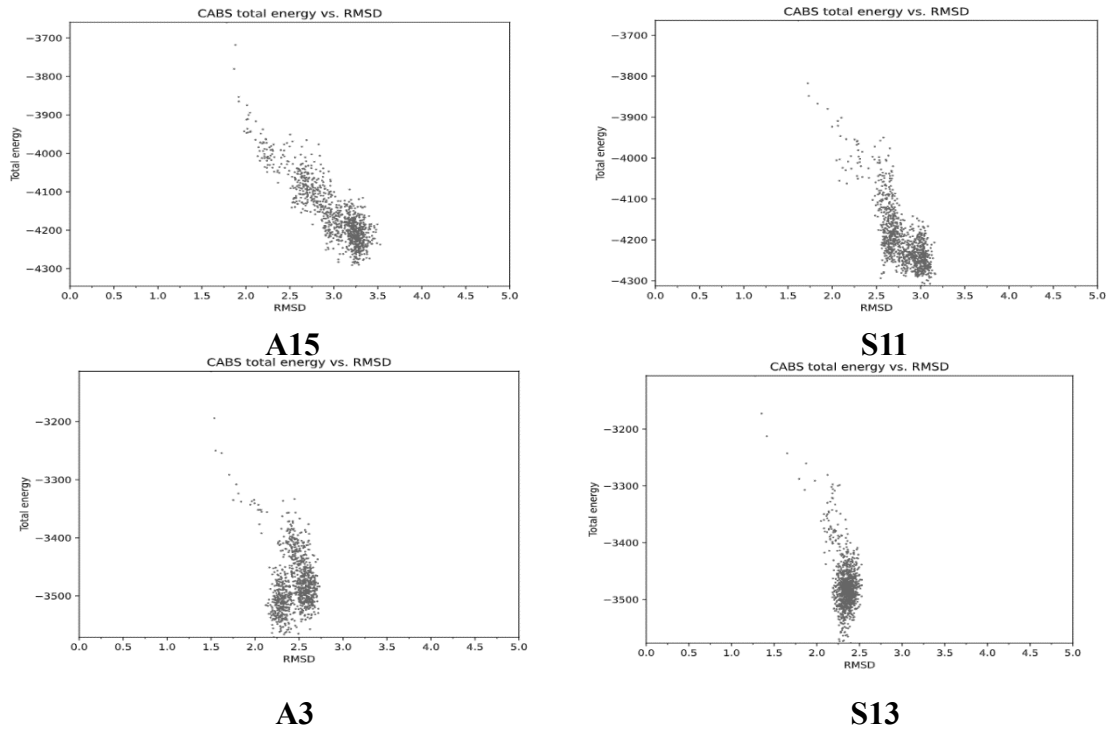

Figure4. CABS-flex simulation analysis showing total energy as a function of RMSD for the selected ligand–protein complexes: (A) A15–4QTD, (B) S11–4QTD, (C) A3–1U6D, and (D) S13–1U6D.

The iMODS normal mode analysis was used in addition to define the inherent flexibility as well as the collective movement of protein-ligand complexes. This analysis included deformability plots, B-factor comparisons, eigenvalue spectra, variance maps, covariance matrices, as well as elastic network analysis. The deformability plots provided insights into the flexibility of individual residues, as well as the peaks representing regions that can undergo greater conformational changes. The B-factor comparison also facilitates the comparison of predicted residue displacement, thus allowing the definition of flexible as well as comparably rigid regions of protein structures.

The eigenvalue spectrum provided information on the energetic requirement associated with the collective motions of the complexes. The variance maps represented the contribution of individual modes to the overall conformational motion, whereas the covariance matrices illustrated correlated and anti-correlated motions between residue pairs. In addition, the elastic network analysis demonstrated the pattern of residue contacts and the corresponding strength of the interactions within the protein structure. Collectively, these iMODS analyses provided complementary information on the dynamic behavior and structural flexibility of the selected complexes (fig.6).

Overall, the combined CABS-flex and iMODS-NMAanalyses supported the assessment of conformational behavior of the selected ligand–protein complexes. The observed clustering of CABS-flex conformations together with the residue flexibility, collective motion, covariance, and elastic-network profiles provided additional structural information following the molecular docking analysis.

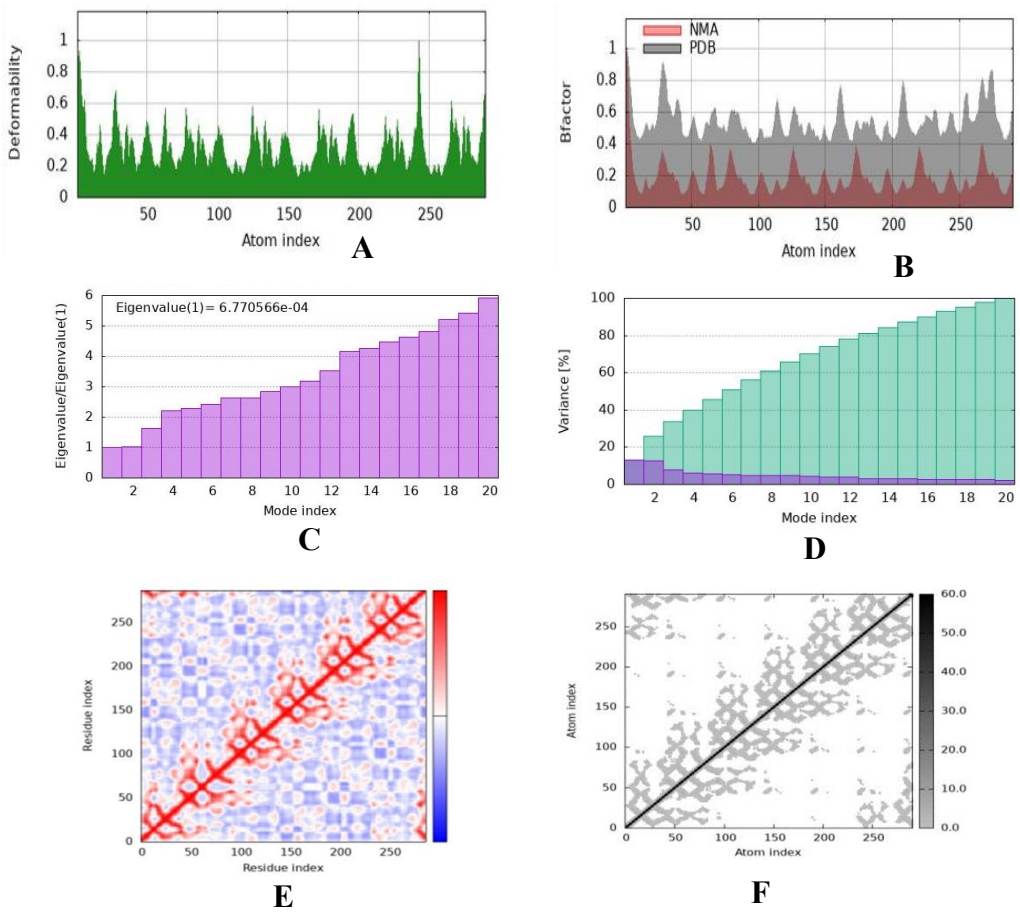

Figure5.iMODS normal mode analysis of the selected ligand–protein complexes with PDB ID: 4QTD showing (A) deformability profile, (B) B-factor comparison, (C) eigenvalue spectrum, (D) variance map, (E) covariance matrix, and (F) elastic network analysis.

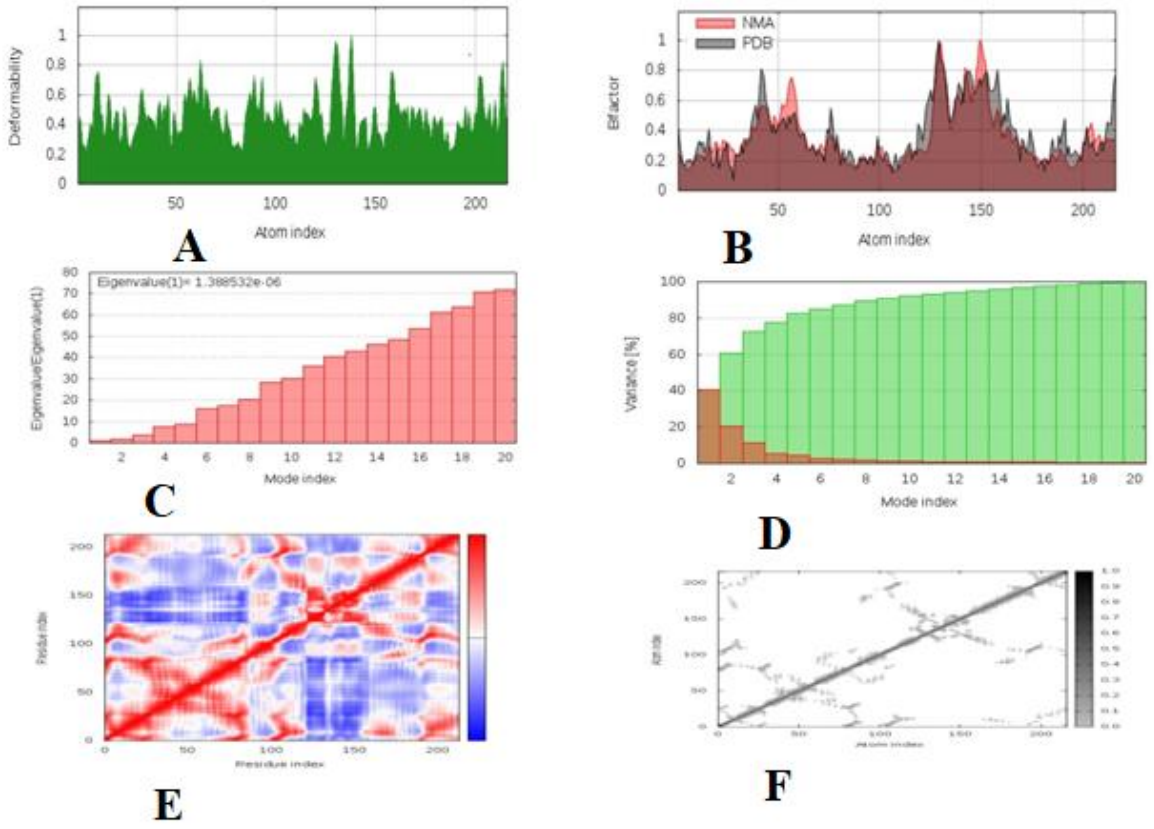

Figure 6: iMODS normal mode analysis of the selected ligand–protein complexes with PDB ID 1U6D showing (A) deformability profile, (B) B-factor comparison, (C) eigenvalue spectrum, (D) variance map, (E) covariance matrix, and (F) elastic network analysis.

4.3 ADME and Toxicity Prediction:

The SwissADME analysis revealed considerable variation in the physicochemical properties of the selected compounds. The molecular weight ranged from 154.25 to 678.42 g/mol, while the TPSA values ranged from 20.23 to 269.43 Å². The predicted ESOL Log S values varied from −8.02 to −0.15, indicating differences in the predicted aqueous solubility of the compounds. The Lipinski rule analysis showed 0–3 rule violations, with several compounds showing no violations, including A7, A10, A15, S3, S4, S5, S8, and S11, as shown in fig.7 and table 3.

The findings from the ProTox toxicity prediction showed hepatotoxicity and neurotoxicity were inactive for almost all compounds analysed, while nephrotoxicity was active for several compounds. Consideration was given to the fact that A2 and S13 were predicted as active for hepatotoxicity, and that S9 was predicted to exhibit activity for nephrotoxicity and neurotoxicity. Overall, the SwissADME and ProTox predictions provided relevant preliminary data on physicochemical properties, solubility, drug-likeness and predicted toxicity profiles of a series of compounds investigated in this research. The information gained through in silico studies was subsequently used to aid the assessment of potential compounds for further studies.

Achyranthes aspera ***Duranta erecta***

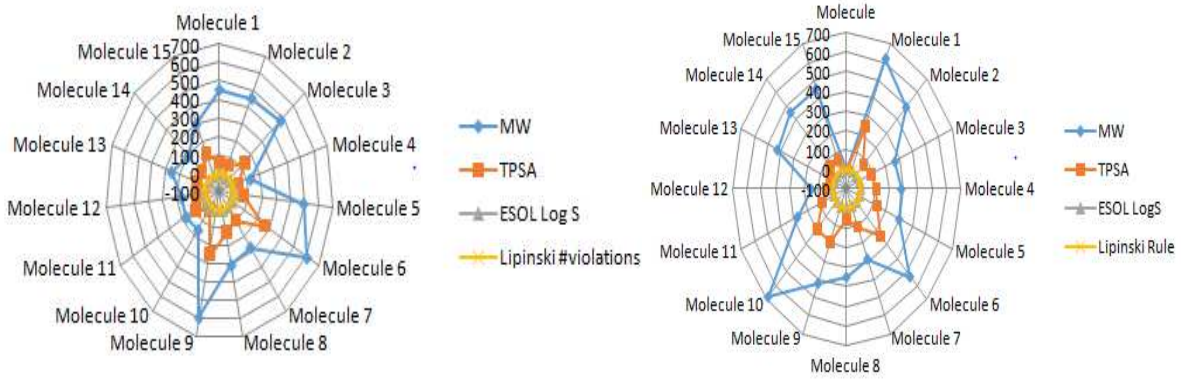

A **B**

Figure7.SwissADME radar plots depicting molecular weight (MW), topological polar surface area (TPSA), ESOL Log S, and Lipinski rule violations of selected compounds from (A) *Achyranthes aspera* and (B) *Durantaerecta*.

Table 3The predicted physicochemical and toxicity profiles of the selected compounds

Sr.No	Molecular Weight	TPSA	ESOL Log S	Lipinski Rules	Hepatotoxicity	Nephrotoxicity	Neurotoxity
Achyranthesaspera							
A1	456.7	57.53	-7.32	1	Inactive	Active	Inactive
A2	456.7	57.53	-7.23	1	Active	Inactive	Inactive
A3	480.63	138.45	-2.78	1	Inactive	Inactive	Inactive
A5	494.77	71.98	-8.02	1	Inactive	Inactive	Inactive
A6	610.52	269.43	-2.33	3	Inactive	Active	Inactive
A7	270.24	90.9	-3.23	0	Inactive	Active	Inactive
A9	594.52	249.2	-2.46	3	Inactive	Active	Inactive
A10	154.25	20.23	-2.78	0	Inactive	Inactive	Inactive
A15	302.24	131.36	-3.19	0	Inactive	Active	Inactive
Durantaerecta							
S1	624.59	245.29	-2.87	3	Inactive	Active	Inactive
S2	494.77	71.98	-8.02	1	Inactive	Inactive	Inactive
S3	270.24	90.9	-3.23	0	Inactive	Active	Inactive
S4	286.24	111.13	-3.07	0	Inactive	Active	Inactive
S5	302.24	131.36	-3.19	0	Inactive	Active	Inactive
S8	349.42	57.61	-4.63	0	Inactive	Active	Inactive
S9	422.38	195.6	-0.15	2	Inactive	Active	Active

S10	678.42	190.67	-3.71	2	Inactive	Active	Inactive
S11	272.25	86.99	-3.49	0	Inactive	Active	Inactive
S13	456.7	57.53	-7.32	1	Active	Active	Inactive

5. Conclusion:

The integrated structure-based in silico method has been utilized in this research to evaluate derivatives of Achyranthes aspera and Durantaerecta against the proteins involved in the paracetamol-induced hepatotoxicity in the liver. The docking results involving Keap1 (PDB id: 1U6D) and JNK1/MAPK8 (PDB id: 4QTD) show good binding of certain selected molecules involving hydrogen bonding, π-interactions, and other non-covalent interactions with various critical amino acids in the binding sites. Among all of the selected derivatives, compounds A3, A9, A2, and S13 showed very good docking scores for 1U6D protein while S11, S1, and S2 had good results with 4QTD. The standard drugs also showed good binding with the proteins. The SwissADMEanalysis showed variation in the physicochemical and drug-likeness characteristics of the selected compounds, with molecular weights ranging from 154.25 to 678.42 g/mol**,** TPSA values from 20.23 to 269.43 Å^2**,** and ESOL Log S values from −8.02 to −0.15**.** The Lipinski analysis showed 0–3 rule violations across the investigated compounds. ProToxprediction provided preliminary toxicity profiles, with most compounds predicted to be inactive for hepatotoxicity and neurotoxicity, although nephrotoxicity was predicted for several compounds. Furthermore**,** CABS-flex analysis showed clustered conformational distributions for the selected complexes. The A15–4QTD and S11–4QTD complexes predominantly occupied RMSD ranges of approximately 2.5–3.3 Å and 2.5–3.1 Å, respectively, whereas A3–1U6D and S13–1U6D showed major conformational populations around 2.3–2.9 Å and 2.1–2.6 Å**,** respectively. The corresponding total-energy profiles showed predominantly lower-energy conformations within the major clusters. Additionally, iMODS-NMA analysis provided information on residue deformability, B-factor distribution, eigenvalue profiles, variance, correlated and anti-correlated motions, and elastic-network interactions, further supporting the conformational and dynamic assessment of the selected ligand–protein complexes. The computational analyses revealed complementary information about various compounds of Achyranthes aspera and Durantaerecta that could be suitable candidates for hepatoprotective drugs. Since the results of docking, predicted toxicity, and structure stability obtained from the analyses indicate potential, further studies should be carried out in regard to the two species. However, this study is based on computational predictions and has to be verified through systematic in vitro or in vivo studies to evaluate the effectiveness, mechanism of action, and safety of these compounds.

Acknowledgement: We express our sinceres gratitude to almighty and Head of Department (Pharmacy) MJP Rohilkhand University Bareilly for providing guidance throughout this study.

Author Contributions: Shreya Gupta: Writing-original draft, Pawan Kumar Gupta: Validation, Nandani Sharma, Kamini, Yogesh Kumar**:** Review and Editing, Shashi Bhooshan Tiwari: Supervision, Conceptualization.

Conflict of interest: The authors declare that they have no known competing financial interests or personal relationships that could have influenced the work reported in this manuscript.

Data Availability Statement: The datasets generated during and/or analysed during the current study are available from the corresponding author on reasonable request.

Funding: None

Conflict of Interest: None

Ethics, Consent to Participate, and Consent to Publish declarations: Not applicable

Clinical Trial Number: Not applicable

References:

1. Ozougwu, J. C. (2017). Physiology of the liver. *International Journal of Research in Pharmacy and Biosciences, 4*(8), 13–24.
2. Alamri, Z. Z. (2018). The role of liver in metabolism: An updated review with physiological emphasis. *International Journal of Basic & Clinical Pharmacology, 7*(11), 2145–2152. https://doi.org/10.18203/2319-2003.ijbcp20184211.
3. Tang, Q., Li, J., Song, H., Zhang, A., Zeng, H., Xu, Y., Mo, L., & He, J. (2026). Hypothalamic control of liver health and disease: From circuits to pathophysiology and therapies. *Advanced Science*. https://doi.org/10.1002/advs.76747.
4. Aslam, A., &Kwo, P. Y. (2023). Epidemiology and disease burden of alcohol-associated liver disease. *Journal of Clinical and Experimental Hepatology, 13*(1), 88–102. https://doi.org/10.1016/j.jceh.2022.09.001.
5. Yang, Y., Li, L., & Wang, X. (2021). Environmental risk factors implicated in liver disease: A mini-review. *Frontiers in Public Health, 9*, 683719. https://doi.org/10.3389/fpubh.2021.683719.
6. Yang, J. D., Hainaut, P., Gores, G. J., Amadou, A., Plymoth, A., & Roberts, L. R. (2019). A global view of hepatocellular carcinoma: Trends, risk, prevention and management. *Nature Reviews Gastroenterology &Hepatology, 16*, 589–604. https://doi.org/10.1038/s41575-019-0186-y.
7. Raschi, E., & De Ponti, F. (2019). Strategies for early prediction and timely recognition of drug-induced liver injury: The case of cyclin-dependent kinase 4/6 inhibitors. *Frontiers in Pharmacology, 10*, 1235. https://doi.org/10.3389/fphar.2019.01235.
8. Andrade, R. J., Chalasani, N., Björnsson, E. S., Suzuki, A., Kullak-Ublick, G. A., Watkins, P. B., Devarbhavi, H., Merz, M., Lucena, M. I., Kaplowitz, N., &Aithal, G. P. (2019). Drug-induced liver injury. *Nature Reviews Disease Primers, 5*, 58. https://doi.org/10.1038/s41572-019-0105-0.
9. Andrade, R. J., Chalasani, N., Björnsson, E. S., Suzuki, A., Kullak-Ublick, G. A., Watkins, P. B., Devarbhavi, H., Merz, M., Lucena, M. I., Kaplowitz, N., &Aithal, G. P. (2019). Drug-induced liver injury. *Nature Reviews Disease Primers, 5*, 58. https://doi.org/10.1038/s41572-019-0105-0.
10. LeFort, K. R., Rungratanawanich, W., & Song, B.-J. (2024). Contributing roles of mitochondrial dysfunction and hepatocyte apoptosis in liver diseases through oxidative stress, post-translational modifications, inflammation, and intestinal barrier dysfunction. *Cellular and Molecular Life Sciences, 81*, 34. https://doi.org/10.1007/s00018-023-05061-7.

11. Villanueva-Paz, M., Morán, L., López-Alcántara, N., Freixo, C., Andrade, R. J., Lucena, M. I., &Cubero, F. J. (2021). Oxidative stress in drug-induced liver injury (DILI): From mechanisms to biomarkers for use in clinical practice. *Antioxidants, 10*(3), 390. https://doi.org/10.3390/antiox10030390.
12. Jaeschke, H., & Ramachandran, A. (2024). Acetaminophen hepatotoxicity: Paradigm for understanding mechanisms of drug-induced liver injury. *Annual Review of Pathology: Mechanisms of Disease, 19*, 453–478. https://doi.org/10.1146/annurev-pathmechdis-051122-094016.
13. Tiwari, D. (n.d.). *Mechanistic insights into the hepatoprotective activity of Terminalia arjuna* [Master's thesis, Indraprastha Institute of Information Technology Delhi]. IIIT-Delhi Institutional Repository. http://repository.iiitd.edu.in/xmlui/handle/123456789/1902.
14. Mohi-ud-din, R., Mir, R. H., Sawhney, G., Dar, M. A., & Bhat, Z. A. (2019). [Article title]. *Current Drug Metabolism, 20*(11), 867–879. https://doi.org/10.2174/1389200220666191105121653.
15. Chen, W., Zhu, J., & Li, S. (2024). Role of c-Jun N-terminal kinase (JNK) signaling pathway in acetaminophen hepatotoxicity. *Authorea*. https://doi.org/10.22541/au.170668618.89998940/v1.
16. Sun, T., & Ye, L. (2026). Research progress on the protective effect and oxidative stress mechanism of rutin against liver injury. *Molecular Medicine Reports*, Article 271. https://doi.org/10.3892/mmr.2026.13982.
17. Akakpo, J. Y., Ramachandran, A., Curry, S. C., Rumack, B. H., &Jaeschke, H. (2022). Comparing *N*-acetylcysteine and 4-methylpyrazole as antidotes for acetaminophen overdose. *Archives of Toxicology, 96*(2), 453–465. https://doi.org/10.1007/s00204-021-03211-z.
18. Janković, S. M. (2022). Acetaminophen toxicity and overdose: Current understanding and future directions for NAC dosing regimens. *Expert Opinion on Drug Metabolism & Toxicology, 18*(11), 745–753. https://doi.org/10.1080/17425255.2022.2151893.
19. Ndhlala, A. R., Ghebrehiwot, H. M., Ncube, B., Aremu, A. O., Gruz, J., Šubrtová, M., Doležal, K., du Plooy, C. P., Abdelgadir, H. A., & Van Staden, J. (2015). Antimicrobial, anthelmintic activities and characterisation of functional phenolic acids of *Achyranthes aspera* Linn.: A medicinal plant used for the treatment of wounds and ringworm in East Africa. *Frontiers in Pharmacology, 6*, 274. https://doi.org/10.3389/fphar.2015.00274.
20. Nargatti, P., Patil, S., &Wadkar, K. (2021). Phytochemical profile and pharmacological aspects of *Achyranthes aspera* Linn—An overview. *Journal of Pharmaceutical Research International, 33*(34B), 187–206. https://doi.org/10.9734/jpri/2021/v33i34B31802.
21. Udobi, M. I., Nzeakor, T. A., Eke, I. G., Ezeh, I. O., Onyeabor, A., Idika, I. K., &Nwosu, C. O. (2018). Evaluation of the anthelmintic potential of *Durantaerecta* L. (Verbenaceae) fruits used in Nigerian ethnomedicine as a vermifuge. *Journal of Ethnopharmacology*. https://doi.org/10.1016/j.jep.2018.01.030.
22. Shaheen, S., Usman, N., Siddique, R., Alhomaidi, E., Khalid, S., Khalid, Z., Sonia, R., Ibadullayeva, S., Dinislam, K., &Mursal, N. (2025). Microscopic and analytical insights into the morphoanatomical, pharmacognosy and bioactivity of healthy and geminivirus-infected *Durantaerecta* L.: A new report. *Journal of Phytopathology, 173*(5), e70165. https://doi.org/10.1111/jph.70165.

23. Srivastava, M., Singh, M., Maurya, P., Srivastava, N., Gupta, N., &Shanker, K. (2019). Simultaneous quantification of five bioactive phenylethanoid, iridoid, and flavonol glycosides in *Durantaerecta* L.: Ultra performance liquid chromatography method validation and uncertainty measurement. *Journal of Pharmaceutical and Biomedical Analysis, 172*, 96–104. https://doi.org/10.1016/j.jpba.2019.06.044.
24. Murmu, S., Aravinthkumar, A., Singh, M. K., Sharma, S., Das, R., Jha, G. K., Prakash, G., Rana, V. S., Kaushik, P., &Farooqi, M. S. (2025). Identification of potent phytochemicals against *Magnaportheoryzae* through machine learning aided-virtual screening and molecular dynamics simulation approach. *Computers in Biology and Medicine*. https://doi.org/10.1016/j.compbiomed.2025.109862.
25. Halder, S. K., Sultana, I., Shuvo, M. N., Shil, A., Himel, M. K., Hasan, M. A., &Shawan, M. M. A. K. (2023). In silico identification and analysis of potentially bioactive antiviral phytochemicals against SARS-CoV-2: A molecular docking and dynamics simulation approach. *Journal of Chemistry, 2023*, 5469258. https://doi.org/10.1155/2023/5469258.
26. Elayyan, A. E. M., Elasbali, A. M., Alanazi, M. A. M., Shamsi, A., & Mohammad, T. (2025). Identification of bioactive phytoconstituents as promising ABL2 inhibitors using virtual screening and molecular dynamics simulation. *Scientific Reports, 15*, 44528. https://doi.org/10.1038/s41598-025-28195-z.
27. Ali, M., Asghar, E., Ali, W., Mustafa, G., Ansari, I. A., Zia, S., Ansari, S. A., & Khan, S. (2024). Screening of multitarget compounds against acetaminophen hepatic toxicity using in silico, in vitro, and in vivo approaches. *Molecules, 29*(2), 428. https://doi.org/10.3390/molecules29020428.
28. Shawky, A. R., Metwaly, H. A., Ragab, H. M., & Wahid, A. (2026). Fused azine derivatives mitigate long-term paracetamol-induced liver fibrosis in mice: Role of JNK1/ASK1 and Nrf2/HO-1 signaling pathways. *Inflammation, 49*(1), 186. https://doi.org/10.1007/s10753-026-02579-3.
29. Mohammed, A. E., Alghamdi, S. S., Shami, A., Suliman, R. S., Aabed, K., Alotaibi, M. O., et al. (2023). In silico prediction of *Malvaviscusarboreus* metabolites and green synthesis of silver nanoparticles—Opportunities for safer anti-bacterial and anti-cancer precision medicine. *International Journal of Nanomedicine, 18*, 2141–2162. https://doi.org/10.2147/IJN.S400195.
30. Chaitanya, D. A., et al. (2012). Hepatoprotective effect of biherbalethanolic extract against paracetamol-induced hepatic damage in albino rats. *Journal of Ayurveda and Integrative Medicine, 3*(4), 198–203. https://doi.org/10.4103/0975-9476.104436.
31. Donkor, S., Larbie, C., Komlaga, G., &Emikpe, B. O. (2020). Evaluation of the acute hepatoprotective potential of hydroethanolic extract of *Durantaerecta* L. parts. *Journal of Toxicology, 2020*, 8815719. https://doi.org/10.1155/2020/8815719.
32. Donkor, S. (2025). *Durantaerecta* L. extracts exert hepatoprotective effect on CCl_4-induced toxicity via inactivating NF-κB pathway. *RPS Pharmacy and Pharmacology Reports, 4*(3), rqaf007. https://doi.org/10.1093/rpsppr/rqaf007.
33. Mohammed, A. E., Alghamdi, S. S., Shami, A., Suliman, R. S., Aabed, K., Alotaibi, M. O., et al. (2023). In silico prediction of *Malvaviscusarboreus* metabolites and green synthesis of silver nanoparticles—Opportunities for safer anti-bacterial and anti-cancer precision medicine. *International Journal of Nanomedicine, 18*, 2141–2162. https://doi.org/10.2147/IJN.S400195.

34. Elayyan, A. E. M., Elasbali, A. M., Alanazi, M. A. M., Shamsi, A., & Mohammad, T. (2025). Identification of bioactive phytoconstituents as promising ABL2 inhibitors using virtual screening and molecular dynamics simulation. *Scientific Reports, 15*, 44528. https://doi.org/10.1038/s41598-025-28195-z.
35. Raval B,Ganatra T. (2022) Basics, types and applications of molecular docking: A review, IP International Journal of Comprehensive and Advanced Pharmacology, 7(1), 12-16. https://doi.org/10.18231/j.ijcaap.2022.003.
36. K. Harrouche, N. Boutaoui, K.M. Saidi, M.Z. Stiti, A. Khelafi, S. Khelili, Design, synthesis, and biological evaluation of new ureido (thioureido) anthranilic acid isosteres: Molecular docking, in silico ADMET predictions, and in vivo anti-inflammatory activity, Chem. Biodivers. 22 (2025) e202500374. https://doi.org/10.1002/cbdv.202500374.
37. K. Wróblewski, M. Zalewski, A. Kuriata, S. Kmiecik, CABS-flex 3.0: An online tool for simulating protein structural flexibility and peptide modeling, Nucleic Acids Res. 53 (2025) W95–W101. https://doi.org/10.1093/nar/gkaf412.
38. Kuriata, A.M. Gierut, T. Oleniecki, M.P. Ciemny, A. Kolinski, M. Kurcinski, S. Kmiecik, CABS-flex 2.0: A web server for fast simulations of flexibility of protein structures, Nucleic Acids Res. 46 (2018) W338–W343. https://doi.org/10.1093/nar/gky356.